

**SMALL FIELD DOSIMETRIC VERIFICATION
AND PATIENT SPECIFIC QUALITY ASSURANCE
FOR CYBERKNIFE RADIOSURGERY SYSTEM
USING 3D GEL DOSIMETERS**

MD ABDULLAH AL KAFI

UNIVERSITI SAINS MALAYSIA

2024

**SMALL FIELD DOSIMETRIC VERIFICATION
AND PATIENT SPECIFIC QUALITY ASSURANCE
FOR CYBERKNIFE RADIOSURGERY SYSTEM
USING 3D GEL DOSIMETERS**

by

MD ABDULLAH AL KAFI

**Thesis submitted in fulfilment of the requirements
for the degree of
Doctor of Philosophy**

February 2024

ACKNOWLEDGEMENT

I would like to express my earnest gratitude to Allah SWT for giving me the opportunity to conduct my PhD study and finishing all the requirements. Very special thanks go out to my main supervisor Dr. Mohd Fahmi bin Mohd Yusof for his tireless support and guidance throughout my PhD journey. This thesis would not have possible without his assistance. I would like to express my gratitude to my co supervisors; Dr. Iskandar Shahrin Bin Mustafa and Dr. Mohd Zahri bin Abdul Aziz, Universiti Sains Malaysia, and all other members who helped me in every aspect of the research project. In particular, I would like to thank my field supervisor Dr. Belal Mofteh, King Faisal Specialist Hospital and Research Centre, KSA for his constant guidance and support during the entire course of my research. I would like to thank Dr. Mehenna Arib from King Faisal Specialist Hospital and Research Centre, KSA for his support in measurements, suggestion in writing, and conducting the thesis. I would also like to thank Dr. Akhtar Uzzaman, University Kebangsaan Malaysia for his support, suggestion in writing, and conducting the thesis. I would like to thank my colleague Mamoun Shehadeh for his suggestions and support. Special thanks goes to my wife Monira Khanom who supported and played an important role behind my success. Special thanks also go to my kids; Rayyan Ibn Abdullah, Ridwaan Abdulah and Ahmad Abdullah for their sacrifice and having to cope with my busy schedule during the past few years. I sincerely wish to acknowledge my father late Md Kafil Uddin and my beloved mother Sufia Khatun for laying the foundation of my education. I thank all my brothers, sister, brother-in-law, sister-in-law and parents in law for their constant support, encouragement and being part of my life. I am profoundly grateful to them all.

TABLE OF CONTENTS

ACKNOWLEDGEMENT	ii
TABLE OF CONTENTS	iii
LIST OF TABLES	vi
LIST OF FIGURES	viii
LIST OF SYMBOLS	xiii
LIST OF ABBREVIATIONS	xv
ABSTRAK	xviii
ABSTRACT	xx
CHAPTER 1: INTRODUCTION	1
1.1 Introduction	1
1.2 Problem Statement	5
1.3 Research Objectives	8
1.4 Scope of Research	8
1.5 Thesis Outline	9
CHAPTER 2: LITERATURE REVIEW	10
2.1 Radiation Therapy	10
2.1.1 Linear Accelerator for Radiation Therapy	10
2.1.2 CyberKnife System for Radiation Therapy	12
2.1.3 Absorbed Dose	15

2.1.4	Absolute, Reference and Relative Dosimetry	16
2.1.4 (a)	Absolute Dosimetry	16
2.1.4 (b)	Reference Dosimetry	17
2.1.4(c)	Relative Dosimetry	18
2.1.5	Small Field Detectors	19
2.1.5 (a)	Ionization Chamber	19
2.1.5 (b)	Diode Detectors	20
2.1.5 (c)	Diamond Detectors	21
2.1.5 (d)	Scintillation Detectors	23
2.1.5 (e)	Film Detectors	26
2.1.5 (f)	3D gel Dosimeters	28
2.1.5 (g)	Monte Carlo Simulation	32
2.1.6	Field Output Factors	33
2.1.7	Patient Specific Quality Assurance	39
2.2	Summary of the Previous Studies	49
CHAPTER 3: METHODOLOGY		54
3.1	Field Output Factors for CyberKnife	54
3.1.1	Experimental Setup, Measurements and Simulation for Field Output Factor	55
3.1.2	Uncertainty over Field Output Factor Measurement	63

3.2	Patient Specific Quality Assurance	64
3.2.1	Experimental Setup for Patient Specific Quality Assurance	64
CHAPTER 4: RESULTS AND DISCUSSION		71
4.1	Uncertainty over Detector's Response	71
4.2	Field Output Factors	76
4.3	Patient Specific Quality Assurance	88
CHAPTER 5: CONCLUSIONS AND RECOMMENDATIONS		106
5.1	Conclusion	106
5.1.1	Field Output Factor	106
5.1.2	Patient Specific Quality Assurance	107
5.2	Recommendations for Future Works	108
5.3	Limitations of the Study	109
REFERENCES		110
ETHICAL CONSIDERATIONS		
LIST OF PUBLICATIONS		

LIST OF TABLES

		Page
Table 2.1	The summary of the concepts of absolute, reference and relative dosimetry in different aspects.	18
Table 2.2	The summary of the physical characteristics of the small field detectors used in this study.	25
Table 2.3	The summary on the previous studies done for the FOFs and PSQA for CK system.	50
Table 4.1	Uncertainty over the response of the detectors (Type B) calculated at one standard deviation (1σ).	71
Table 4.2	Standard Errors for measurements with different detectors.	72
Table 4.3	Uncertainty (U) over Ω for the Edge Detector.	73
Table 4.4	Uncertainty (U) over Ω for the PinPoint ionization chamber.	74
Table 4.5	Uncertainty (U) over Ω for the PTW diamond detector.	75
Table 4.6	Standard Errors for the measurements with GafChromic EBT3 films, 3D polymer gel and MC simulation.	75
Table 4.7	MC simulated FOFs (Ω), corresponding uncertainties and their percentage difference with Moignier et al., 2014.	77
Table 4.8	FOFs, their percentage difference with MC and corresponding uncertainty for Sun Nuclear Edge detector.	79
Table 4.9	FOFs, their percentage difference with MC and corresponding uncertainty for PTW diode (TM 60016).	80
Table 4.10	FOFs, their percentage difference with MC and corresponding uncertainty for PTW diamond detector (TM 60003).	80
Table 4.11	FOFs, their percentage difference with MC and corresponding uncertainty for PinPoint (TM 31016) ionization chamber in PMMA.	82

Table 4.12	FOFs, their percentage difference with MC and corresponding uncertainty for PinPoint (TM 31006) ionization chamber in water.	82
Table 4.13	FOFs, their percentage difference with MC and corresponding uncertainty for PTW Semiflex ionization chamber (TM 31010).	83
Table 4.14	FOFs, their percentage difference with MC and corresponding uncertainty for W1 type PSD.	84
Table 4.15	FOFs, their percentage difference with MC and corresponding uncertainty for W2 type PSDs.	84
Table 4.16	FOFs, their percentage difference with MC and corresponding uncertainty for GafChromic EBT3 film and 3D polymer gel.	86
Table 4.17	Results of 2D gamma ($\% \Delta D / DTA$) passing rates for PSQA using GafChromic EBT3 films.	101
Table 4.18	Results of 3D gamma ($\% \Delta D / DTA$) passing rates for PSQA using 3D gel.	102
Table 4.19	Comparison of 2D gamma of EBT3 films to 3D gamma of 3D gel for different $\% \Delta D / DTA$ and cut off doses.	103

LIST OF FIGURES

		Page
Figure 2.1	Schematic diagram of the main components of a typical medical LINAC.	11
Figure 2.2	A typical CK modality (Accuray VSI system used for this study).	13
Figure 2.3	Main Components of CK system.	14
Figure 2.4	A PTW PinPoint ionization chamber (PTW-Freiburg, Germany).	20
Figure 2.5	A PTW Diode 600016 (PTW-Freiburg, Germany).	21
Figure 2.6	A PTW natural diamond detector (PTW-Freiburg, Germany).	22
Figure 2.7	An Extradin W2 Scintillation detector (Standard Imaging Inc., Madison, WI, USA).	24
Figure 2.8	GafChromic EBT3 film (Ashland, Ky, USA) (a) in boxes and (b) on PMMA solid a water slab.	27
Figure 2.9	Irradiated gels in different types of phantoms (a) in small bottles, (b) in plastic cylinders and (c) in a glass jar.	30
Figure 2.10	Hitachi Double Beam Spectrophotometer readout diagram.	32
Figure 2.11	Schematic illustration of source occlusion (a) the full, extended source can be viewed by an observer on the central axis and (b) only a partial view of the source on the central axis is possible.	36
Figure 2.12	The penumbra in relation to the FWHM (a) For sufficiently large field sizes, the FWHM of dose profiles is used correctly to determine field sizes. (b) When the field size is of the same order as the charged particle lateral diffusion distance, the penumbra region from opposing field edges overlap, leading to a small error in determining the field size from the FWHM, (c) but breaks down entirely for very small fields as the	37

obtained curve has a lower maximum and hence its half value will be pushed outward from the correct position, leading to an overestimated field size.

Figure 2.13	Volume averaging effect (a) flattened beam profile with large detector and (b) spreading of the penumbra with larger detector than smaller one.	37
Figure 2.14	CrystalBall gel phantom PSQA system (a) CrystalBall gel phantom and (b) PMMA QA stand.	46
Figure 2.15	CrystalBall gel phantom PSQA system (a) and (b) CrystalBall gel phantom mounted on an Acrylic QA stand.	47
Figure 2.16	OCTOPUS LCT scanning system (MGS Research, Inc., Madison, CT, USA).	47
Figure 2.17	OCTOPUS LCT scanning system schematic readout diagram.	48
Figure 3.1	An ionization chamber setup in PTW water phantom (PTW, Freiburg, Germany).	55
Figure 3.2	Film strips for calibration (a) on Solid Water Phantom under CK treatment head (b) Irradiated calibration films on an EPSON scanner.	57
Figure 3.3	An EPSON EXPRESSION 11000 XL scanner (a) front cover closed and (b) front cover opened (Epson America, Inc., USA).	57
Figure 3.4	EBT2 film calibration curve for CK FOF calculations.	58
Figure 3.5	Cuvette for 3D gel (a) an empty cuvette and (b) irradiated gel in cuvettes.	59
Figure 3.6	Spectrophotometer readout (a) a Double Beam Spectrophotometer (b) an irradiated cuvette in the Spectrophotometer (Hitachi, Ltd., Japan).	59
Figure 3.7	MC simulation model of CK LINAC head with 60 mm cone.	61

Figure 3.8	Measured vs MC calculated PDDs for 60 mm, 25 mm, 10 mm and 5 mm cones.	62
Figure 3.9	Treatment plan for a CK patient from Accuray Multiplan TPS.	65
Figure 3.10	A treatment plan superimposed on the CrystalBall gel phantom; (a) merged 3D patient model with model 3D CrystalBall model (green treatment beams are also visible), (b) superimposed 2D treatment plan along with the 2D isodose lines on axial CT of both, (c) on sagittal CT and (d) on coronal CT for a brain metastasis patient.	66
Figure 3.11	3D gel autocalibration (a) optical density per centimeter (OD/cm) to dose auto calibration curve and (b) the polynomial fit for the calibration for a brain metastasis patient.	67
Figure 3.12	EBT3 film sandwiched inside solid water slabs.	69
Figure 3.13	A treatment plan superimposed on the film-PMMA slab phantom (a) merged 3D patient model with film-PMMA slabs (b) superimposed 2D treatment plan along with the 2D isodose lines on axial CT of both (c) on sagittal CT and (d) coronal CT for a brain metastasis patient.	69
Figure 3.14	An irradiated EBT3film on solid water slabs in CK.	70
Figure 4.1	FOFs for different MC simulations.	78
Figure 4.2	FOFs for MC simulation, Sun Nuclear Edge detector, PTW diode and PTW Diamond detector.	81
Figure 4.3	FOFs for MC simulation, PTW PinPoint and Semiflex ionization chambers.	83
Figure 4.4	FOFs for MC simulation and PSDs (W1 and W2).	85
Figure 4.5	FOFs for MC simulation, GafChromic EBT3 film and 3D gel.	86
Figure 4.6	Axial planned vs measured overlays of 2D isodose lines through Dmax for one of the patients studied.	89

Figure 4.7	Coronal planned vs measured overlays of 2D isodose lines through Dmax for one of the patients studied.	89
Figure 4.8	Sagittal planned vs measured overlays of 2D isodose lines through Dmax for one of the patients studied.	90
Figure 4.9	Planned vs measured 3D overlays of 30% isodose surfaces for one of the patients studied.	90
Figure 4.10	Planned vs measured 3D overlays of 50% isodose surfaces (the isodose surfaces are zoomed to make the fine details better visible).	91
Figure 4.11	Planned vs measured 3D overlays of 70% isodose surfaces (the isodose surfaces are zoomed to make the fine details better visible).	91
Figure 3.12	Planned vs measured 3D overlays of 80% isodose surfaces (the isodose surfaces are zoomed to make the fine details better visible).	92
Figure 4.13	Planned vs measured A-P profiles for %Dose/DTA (mm)/Sigma (Gamma) through Dmax for a brain metastasis patient studied.	92
Figure 4.14	Planned vs measured R-L profiles for %Dose/DTA (mm)/Sigma (Gamma) through Dmax for a brain metastasis patient studied.	93
Figure 4.15	Planned vs measured I-S profiles for %Dose/DTA (mm)/Sigma (Gamma) through Dmax for a brain metastasis patient studied.	93
Figure 4.16	Planned vs measured cumulative dose volume histogram for 3D structures defined by some selected isodose surfaces for a patient studied.	94
Figure 4.17	The raw LCT 2D dose map (a) planned and (b) measured for a spine metastasis patient using ImageJ software.	95

Figure 4.18	The intensity profiles (a) planned and (b) measured for a spine metastasis patient as indicated in Figure 4.17 using ImageJ software.	95
Figure 4.19	Superimposed (upper curve) planned vs measured raw 2D intensity profiles through a selected plane for a spine metastasis patient (as in figure 4.18) and corresponding percentage difference between the same data points for the planned and measured (lower curve).	96
Figure 4.20	Planned vs measured raw dose for visual comparison (a) planned dose from CK Multiplan and (b) irradiated EBT3 film for a brain metastasis patient.	96
Figure 4.21	Planned vs measured dose using PTW Verisoft for a brain metastasis patient (a) planned dose from TPS and (b) measured EBT film dose.	97
Figure 4.22	Planned vs measured L-R (left-right) dose profile as observed in Figure 4.21.	97
Figure 4.23	Planned vs measured T-G (target-gantry) dose profile as observed in Figure 4.21.	98
Figure 4.24	2D colorwash for (a) planned and (b) measured isodoses for EBT3 film using PTW Verisoft.	98
Figure 4.25	Planned vs measured 2D isodose overlays using PTW Verisoft.	99
Figure 4.26	Passed and failed evaluation points for a patient using PTW Verisoft.	99
Figure 4.27	2D gamma map for EBT3 film for a patient using PTW Verisoft.	100
Figure 4.28	2D gamma evaluation report for EBT3 film for patient using PTW Verisoft.	101

LIST OF SYMBOLS

A	Absorbance
$_{clin}$	Clinical
De	Evaluated dose
Dr	Reference dose
I	Intensity (final)
I_0	Intensity (initial)
Ω	Field Output Factor
ϵ	Energy Imparted
m	Mass of a medium
$_{msr}$	Machine Specific reference
Γ	Gamma
γ	Gamma passing rate
σ	Standard Deviation
\vec{r}_e	Position vector for evaluated point
\vec{r}_r	Position vector for reference point
\log_{10}	logarithm with base 10
f_{clin}	Clinical field
f_{msr}	Machine specific reference field
Q_{clin}	Clinical beam quality
Q_{msr}	Machine specific reference beam quality
$k_{Q_{clin}^{f_{clin}}/Q_{msr}^{f_{msr}}}$	Output correction factor for a clinical beam relative to the machine specific reference field

$M_{Q_{clin}}^{f_{clin}}$	Detector reading in the clinical field in a clinical beam quality, corrected for influence quantities
$M_{Q_{msr}}^{f_{msr}}$	Detector reading in the machine specific reference field in a machine specific reference beam of quality, corrected for influence quantities
$\Omega_{Q_{clin}, Q_{msr}}^{f_{clin}, f_{msr}}$	Field output factor for a clinical field relative to the machine specific reference field
T	Transmittance
U	Overall uncertainty

LIST OF ABBREVIATIONS

3D	Three Dimensional
AAPM	American Association for Physicists in Medicine
ACR	American College of Radiology
ASTRO	American Society for Radiation Oncology
CIRMS	The Council on Ionizing Radiation Measurements and Standards
CK	CyberKnife
CLR	Cherenkov light radiation
CoP	Code of Practice
CPE	Charged Particle Equilibrium
CRT	Conventional Radiation Therapy
CVD	Chemical Vapor Deposition
CT	Computed Tomography
ΔD	Dose Difference
DICOM	Digital Imaging and Communications in Medicine
DTA	Distance to Agreement
ECUT	Electron Cut-off Energy
eV	Electron Volt
FFF	Flattening Filter Free
FOF	Field Output Factor
FWHM	Full Width at Half Maximum
IAEA	International Atomic Energy Agency
IGRT	Image Guided Radiation Therapy
IMRT	Intensity Modulated Stereotactic Radiation Therapy

IPEM	The Institute of Physics and Engineering in Medicine
LCPE	Lateral Charged Particle Equilibrium
L-R	Left-Right
LCT	Laser Coherence Tomography
LINAC	Linear Accelerator
MC	Monte Carlo
MRI	Magnetic Resonance Imaging
MU	Monitor Unit
MV	Mega Volt
NIST	The National Institute of Standards and Technology
NMR	Nuclear Magnetic Resonance
NPL	The National Physical Laboratory
OCT	Optical Coherence Tomography
OD	Optical Density
OF	Output Factor
PCUT	Photon Cut-off Energy
PDD	Percentage Depth Dose
PMMA	Poly(methyl methacrylate)
PRF	Pulse Repetition Frequency
PSD	Plastic Scintillation Detector
PSDL	Primary Standard Dosimetry Laboratory
PSQA	Patient Specific Quality Assurance
PTB	Physikalisch-Technische Bundesanstalt
QA	Quality Assurance
SAD	Source to Axis Distance

SBRT	Stereotactic Body Radiation Therapy
SCDDo	Single Crystal Diamond Dosimeter
SRS	Stereotactic Radiosurgery
SRT	Stereotactic Radiation Therapy
TG	Task Group
T-G	Target-Gantry
TRS	Technical Report Series
TPS	Treatment Planning System
VMAT	Volumetric Arc Therapy

**PENGESAHAN DOSIMETRI MEDAN KECIL DAN JAMINAN
KUALITI KHUSUS PESAKIT RADIOSURGERI CYBERKNIFE
MENGUNAKAN DOSIMETER GEL 3D**

ABSTRAK

Sistem Robotik CyberKnife (CK) radioterapi/radiosurgeri stereotaktik menggunakan sinaran dengan keamatan yang modulasi atau saiz medan yang sangat kecil untuk merawat tumor yang mempunyai kecerunan dos yang tinggi. Untuk mengatasi kekangan untuk dosimetri medan yang kecil tersebut, volum kecil, resolusi tinggi dan pengesan sinaran yang setara dengan tisu adalah disyorkan. Kod amalan antarabangsa (CoP) gabungan antara International Atomic Energy Agency (IAEA) dan American Association of Physics in Medicine (AAPM), iaitu kod TRS 483 telah menyediakan garis panduan pengukuran faktor keluaran medan (FOF) dan faktor pembetulan keluaran medan untuk siri pengesan bagi medan kecil. Kod amalan ini mengesyorkan lebih banyak pengukuran tambahan dan pengumpulan data menggunakan pengesan sedia ada dan yang baharu untuk sistem CK. Kajian ini memberi tumpuan kepada penggunaan polimer gel 3D, filem dosimeter EBT3, simulasi Monte Carlo dan beberapa pengesan lain yang tersedia secara komersial untuk pengukuran dan pengesahan FOF untuk medan kecil yang terdapat dalam sistem CK. Perbandingan dengan data Monte Carlo mendapati perbezaan peratusan maksimum bagi faktor pengeluaran medan bagi pengesan sisi diod dan PTW masing-masing ialah 0.99% dan 0.96% untuk kon bersaiz 0.75 cm, serta 3.33% bagi pengesan berlian untuk kon bersaiz 0.50 cm. Untuk kebuk pengionan Pinpoint, peratus perbezaan maksimum ialah sebanyak 1.72% untuk kon bersaiz 0.75 cm apabila disukat dalam air serta sebanyak 2.4% untuk kon bersaiz 1.25 cm di dalam kebuk Semiflex. Peratus perbezaan

maksimum untuk semua pengesanan pandarkilau plastik ialah 1.89%. Untuk filem EBT3, peratus perbezaannya ialah 1.86%, manakala untuk gel polimer 3D ialah 3.93% untuk kon terkecil bersaiz 0.50 cm. Hasil kajian ini telah membuktikan kesesuaian dosimeter polimer gel 3D binaan sendirian, beberapa jenis pengesanan komersial sedia ada, dan filem dosimeter GafChromic EBT3 untuk sistem CK. Untuk pengesanan dan jaminan kualiti (QA) radioterapi ‘hupofractionated stereotactic’ atau rawatan radiosurgeri, teknik dua dimensi dan resolusi rendah lazim didapati tidak mencukupi kerana kecerunan dos yang tinggi di sekeliling tumor. Oleh itu, peralatan beresolusi tinggi dengan keupayaan 3D perlu diperkenalkan bagi pengesanan rawatan tersebut. Kajian ini menggunakan sistem jaminan kualiti khas pesakit (PSQA) polimer gel Radiochromic 3D yang dibangunkan dan dinamakan CrystalBall untuk mengesahkan perancangan rawatan CK. Sejumlah lima belas pesakit CK dengan diagnosis yang berbeza telah dipilih secara rawak dan taburan dos yang diberikan telah dibandingkan dengan kaedah perancangan yang menggunakan kadar 3D penembusan gamma melalui kriteria penerimaan yang dipilih menggunakan perisian VOLQA oleh pengguna. Kadar penembusan gamma gel 3D telah disahkan melalui perbandingan dengan kadar penembusan gamma 2D oleh filem GafChromic EBT3 menggunakan perisian PTW Verisoft. Untuk gel 3D CrystalBall, kadar purata kelulusan indeks gamma untuk perbezaan dos 2% (ΔD) dengan 2 mm jarak yang dipersetujui (DTA) masing-masing ialah $(81.7 \pm 10.3) \%$, $(91.1 \pm 6.4) \%$ dan $(95.6 \pm 3.9) \%$ untuk dos-dos pemisahan 10%, 20% dan 30%. Untuk 3% ΔD dan 3 mm DTA, purata gamma ialah $(89.8 \pm 6.3) \%$, $(96.3 \pm 3.0) \%$ dan $(98.8 \pm 1.1) \%$ masing-masing untuk dos-dos pemisahan 10%, 20% dan 30%. Hasil kajian ini telah membuktikan kesesuaian sistem CrystalBall 3D baharu untuk PSQA sebagai sebahagian daripada jaminan kualiti untuk sistem CK.

**SMALL FIELD DOSIMETRIC VERIFICATION AND PATIENT
SPECIFIC QUALITY ASSURANCE FOR CYBERKNIFE RADIOSURGERY
SYSTEM USING 3D GEL DOSIMETERS**

ABSTRACT

CyberKnife (CK) stereotactic radiotherapy/radiosurgery system uses very small intensity-modulated radiation therapy fields or field segments to treat tumors with high dose gradients. To overcome the limitations for dosimetry of those small fields, small volume, high resolution and tissue-equivalent detectors are recommended. The joint IAEA and AAPM international code of practice (CoP), TRS 483 provides field output factor (FOF) measurement guidelines and field output correction factors for a series of small field detectors. The CoP strongly recommends additional measurements and data collection with available detectors and more new ones for CK. The present study focused on using 3D polymer gel, EBT3 film, Monte Carlo simulation and some other commercially available detectors for the measurement and verification of FOFs for the small field cones (0.50 cm to 60.0 cm) available in CK system. When compared with the Monte Carlo data, the maximum percentage difference for the FOF for Edge detector and PTW diode was found to be 0.99% and 0.96% respectively for 0.75 cm cone, whereas it is 3.33% for diamond detector for 0.50 cm cone. For Pinpoint ionization chamber, the maximum difference is 1.72% for 0.75 cm cone when measured in water and for Semiflex chamber; it is 2.4% for 1.25 cm cone. The maximum difference for all plastic scintillation detectors were 1.89%. For EBT3 film, the difference is 1.86%, whereas it is 3.93% for 3D polymer gel for the smallest 0.50 cm cone. The results of this study have proved the suitability of an in-house built 3D polymer gel dosimeter, several commercially available detectors, and GafChromic

films for the CK system. For the verification and quality assurance (QA) of hypofractionated stereotactic radiotherapy or radiosurgery treatments deliveries, the conventional two dimensional and low resolution techniques are not adequate due to high dose gradient surrounding the tumor. Hence, high resolution tool with 3D capability needs to be introduced those treatment verifications. This study employed a recently developed 3D radiochromic polymer gel patient-specific quality assurance (PSQA) system named CrystalBall to verify CK treatment plans. Fifteen CK patients with different diagnoses were selected randomly and the delivered dose distributions were compared with that of planned by means of 3D gamma passing rates at user-selected acceptance criteria using VOLQA software. The 3D gel gamma passing rates were validated by comparing with GafChromic EBT3 film 2D gamma passing rates using PTW Verisoft software. For 3D CrystalBall gel, the average gamma index passing rates for 2% dose difference (ΔD) and 2 mm distance to agreement (DTA) were $(81.7 \pm 10.3) \%$, $(91.1 \pm 6.4) \%$ and $(95.6 \pm 3.9) \%$ for 10%, 20% and 30% cut-off doses respectively. For 3% ΔD and 3 mm DTA, the average gamma were $(89.8 \pm 6.3) \%$, $(96.3 \pm 3.0) \%$ and $(98.8 \pm 1.1) \%$ for 10%, 20% and 30% cut-off doses respectively. The results of this study have proved the suitability of the new 3D CrystalBall system for PSQA as a part of quality assurance for CK system.

CHAPTER 1

INTRODUCTION

1.1 Introduction

Radiation therapy or radiotherapy uses high-energy radiations like x-rays, electrons or other particles to destroy or damage the tumor or cancer cells while the nearby healthy tissues in the body are spared (National Cancer Institute, 2019). Radiation breaks down the DNA inside cancer cells that ruins their ability to divide or grow and causes them to die while most of the surrounding healthy cells recover and go back to function normally (American Cancer Society, 2019, National Cancer Institute, 2019). Radiation therapy is sometimes adequate as the standalone treatment and other times it is combined with surgery and/or medications such as chemotherapy, hormone therapy and immunotherapy that is commonly known as adjuvant therapy (Park et al., 2012). In case of some advanced cancers, it is used as a palliative treatment that helps to alleviate the symptoms and improve quality of life by reducing the sufferings caused by the cancer (Abshire et al., 2018; Cancer Research UK., 2021). As estimated, more than 50% of the cancer patients will undergo some form of radiation therapy in the whole course of their treatment (Park et al., 2012; American Cancer Society, 2019).

For radiation therapy, usually, a linear accelerator (linac or LINAC) is used to deliver the beam of radiation to the tumor for treatment. For three dimensional conventional radiation therapy (3D CRT), the LINAC delivers radiation to the tumor from various angles with a forward planning approach. A more sophisticated approach was employed with the invention of intensity modulated radiation therapy (IMRT), where the radiation beams can be targeted more precisely to conform the 3D shape of the tumor by modulating the beam intensity in multiple small beams (IMRT

Collaborative Working Group, 2001). Unlike 3D CRT, the dose intensity pattern in IMRT in each field is determined by using computerized dose calculation algorithms to conform to the shape of the tumor by employing inverse planning approach. A more advanced technology, that is the image guided radiation therapy (IGRT) technique incorporated imaging technologies like x-rays, computed tomography (CT) scans and/or magnetic resonance imaging (MRI) scans with IMRT to guide the radiation delivery to the target precisely (Verellen et al., 2008). With the aid of real time imaging, this technique helps to ensure the delivery of radiation more precisely to the target tumor and at the same time minimizes the exposure of radiation to the surrounding healthy tissue (Dawson et al., 2007). Consequently, it can help improve the outcome and reduce side effects for those tumors especially where the tumor and surrounding tissue movement make it difficult for the radiation beam to target precisely. These methods allow us to deliver the radiation in a more targeted and efficient manner.

With new technologies emerging, there has been a growing need for improved and effective cancer treatment with reduced side effect. To provide better outcomes for cancer patients, researchers and healthcare professionals have been constantly working to develop new techniques and simultaneously to improve the existing ones. The CyberKnife (CK) system (Accuray Incorporated, Sunnyvale, CA, USA) is one of such state-of-the-art radiotherapy treatment modalities used for stereotactic radiosurgery/stereotactic radiation therapy/stereotactic body radiation therapy (SRS/SRT/SBRT) treatments for cancerous and noncancerous tumors and some functional disorders. The idea for CK was developed by John Adler, a Stanford-based neurosurgeon in the United States (Adler, 1993; 1996). This treatment is particularly useful for malignancies that are difficult to treat with traditional radiation therapy or

surgery, as it can deliver radiation non-invasively to areas that are hard to reach. Unlike 3D CRT or conventional IMRT, the system is intended to provide very high doses (for tumor ablation) of radiation to the target tumor cells with extreme precision in real-time. With the ability to account for any movement of the tumor or surrounding organs at risk during treatment, CK technology employed a robotic arm to deliver intense radiation doses to the tumor with sub-millimetre accuracy (Wong et al., 2007, Dieterich et al., 2011b). However, any error, even relatively small, if introduced at any stage of the machine acceptance, commissioning or elsewhere in the entire process, may lead to severe consequences in the outcome of the treatment of the patients. The repercussions may include nearby normal healthy tissue complications, recurrences of the tumor, or a partial or complete failure to control of the disease in general. For this reason, accurate dosimetric data collection, measurement, calculation and their proper implementation in the CK system is extremely crucial.

Field output factor (FOF) is a very important dosimetry parameter that is used to calculate the radiation dose delivered to the patient's tumor during treatment. It describes the dose rate of the radiation beam at a specific point in the treatment field. To confirm that the administered dose is consistent with the prescribed dose and to ensure that patients receive precise, safe and effective treatment, accurate dose calculation is immensely essential. An inaccuracy in dose calculation may lead to an overdose or underdose of the target area. Therefore, the accurate measurement and proper implementation of FOF is essential for CK system.

These dosimetric measurements are typically done by using specialized equipments and procedures, and they are integral part of the quality assurance program for CK system. The International Atomic Energy Agency (IAEA) and the American Association of Physicists in Medicine (AAPM) jointly provided guidelines for small

field dosimetry procedures in their technical report series No. 483 (Alfonso et al., 2017). The recommendations for the required characteristics of some commonly available detectors for small field dosimetry as in CK are listed in Table 6 of the CoP. The guidelines for reference and relative dose measurements are also described in various studies (Das et al., 2008a; Aspradakis et al., 2010; Low et al., 2011; Alfonso et al., 2017; Das et al., 2021). They strongly recommended FOF measurements for CK with different detectors currently in use and with new detectors. On that account, this study proposed to investigate and measure FOFs for the CK system with different types of detectors that were commercially available and polymer gel detectors that were developed locally in our institution. The results of all the measurements were compared with the data obtained from Monte Carlo (MC) simulation.

Treatment planning for the patients undergoing treatments in radiation therapy involves determining and calculating the optimal radiation dose and delivery technique for each patient based on their unique anatomy and tumor characteristics. To ensure that the treatment plan is accurate and that the radiation is administered precisely and accurately to the target area, treatment plan verification is necessary. Since CK system uses advanced technology and is intended to deliver high radiation doses to tumors with superior accuracy, without a proper plan quality assurance, there is a substantial risk of delivering high dose of radiation to the healthy tissues and/or missing the target. So high resolution 3D patient specific quality assurance (PSQA) is of great importance in detecting and minimizing errors and to ensure the precise radiation dose delivery to the target volumes for optimal treatment outcome. This study focused on the evaluation of a new polymer gel based PSQA system by using 3D gamma evaluation procedure for CK patients.

1.2 Problem Statement

For the measurements of dosimetric quantities and commissioning of such a sophisticated radiotherapy system like CK, that involves the treatment of SRS/SRT/SBRT, it is crucial to use an accurate dosimetry detector that is low leakage, highly sensitive, stable, dose rate independent, directionally independent, linear response, energy independent with a high spatial resolution and tissue equivalent (Alfonso et al., 2017). A major practical challenge is to measure radiation dose easily and directly in a routinely basis. For accurate measurements of the small fields as used for CK treatments, the detector should also be practically small enough to overcome the so-called volume averaging effect as well as the lateral charge particle equilibrium (LCPE) condition. Depending on the specific needs and preferences, each type of commercially available detector currently in use for small field measurements has its own set of advantages and disadvantages.

Owing to the lack of the availability of an ideal detector for small field dosimetry, several research teams have been investigating different commercially available detectors. The joint AAPM and IAEA CoP, TRS 483 (Alfonso et al., 2017) employed a variety of commercially available detector types for measuring the FOFs for various CK cones and collimators. The CoP provided field output correction factors for some commonly used detectors (that include ion chambers, diode detectors, diamond detectors and scintillator detectors) and recommends them to be applied to the corresponding clinically measured (raw) FOFs to compensate for errors and possible perturbations experienced by the detectors in the medium. In order to maintain a standard for clinical application, not enough studies have been conducted on FOF measurements using all sort of the readily accessible and practicable detectors. There is still a need to establish a standard FOF for CK system to be implemented

clinically. In addition, to ensure effectiveness of the treatment, it is essential to apply appropriate field output correction factors in clinical practice. Otherwise, the risk of unwanted treatment outcomes will be quite high. For this reason, the CoP suggested and stressed further measurements with those detectors to establish standard FOFs for the CK and other radiotherapy modalities. In addition, TRS 483 recommended more measurements with more new types of detectors and techniques with high resolution, tissue equivalence and 3D capability since traditional low resolution measurement techniques and tools are not suitable for small field dosimetric measurements in systems such as CK, as they seem to have limitations and deficiencies. Hence, 3D gel may overcome those limitations.

The International Commission on Radiation Units and Measurements (ICRU, 1978) recommend that radiation dose be delivered within 5% of the prescribed dose. This necessitates that the uncertainty or error in each individual step of the whole treatment process should be minimal. The CK system is designed to deliver very high doses of radiation to the target tumor for intensity modulated and image-guided SRS/SRT/SBRT treatments in a single fraction or much fewer than usual fractionated treatment approach to shorten the overall duration of the treatment course (hypofractionated). Hence, any error, whether relatively small, at any stage in the entire treatment process may lead to underdose of the tumor, an overdose of the tumor and/or surrounding normal healthy tissue. Consequently, a possibility of the tumor future recurrence or severe normal tissue complications or a potential failure to effectively control the disease may not be ruled out (Bogdanich, 2010a; 2010b; Bogdanich et al., 2010; Derreumaux et al., 2011).

To identify and minimize such errors, it is very important for the CK system to implement a process-oriented end-to-end PSQA system to detect and minimize such

errors that may occur during the treatment planning and delivery (Dieterich et al., 2011a; American College of Radiology, 2016; Huq et al., 2016; Halvorsen et al., 2017). The Council on Ionizing Radiation Measurements and Standards (CIRMS 2011) also emphasized the importance of high resolution 3D dosimetry, quality assurance and treatment verification for 3D CRT and IMRT treatments. However, common limitations of most of the PSQA systems in use nowadays are that they usually have low resolution and use 2D arrays of diodes or ion chambers (Spezi et al., 2005; Ileana et al., 2010; Lin et al., 2015; Chan et al., 2021; Xu et al., 2021; Das et al., 2022; Guo et al., 2023; Wei et al., 2023; Xu et al., 2023). These arrays are flat or curved and measure dose distribution in a plane or in an arc. Some of them can be operated standalone and the others are embedded in phantoms. Small volume single point dose measurements are also performed with the help of a single detector (Koksal et al., 2018a; De Martin et al., 2021). Nevertheless, the inherent high dose gradients for SRS/SRT/SBRT treatment fields in CK make it immensely difficult to measure accurate 3D dose distributions with those conventional single point or 2D array dosimeters currently in use. The drawbacks in using the current dosimeters are that they have relatively larger size which causes partial volume averaging effects and lack of electronic equilibrium. Hence, for high resolution measurements and verification of SRS/SRT/SBRT treatment plans as in CK, it is crucial to find out an appropriate three-dimensional dosimetry system, which is independent of dose rate. For the routine use of such a system, a simple and easy phantom setup is desirable. Moreover, the system should be able to generate three dimensional PSQA results as soon as practically possible in a clinical setup following the QA phantom exposure. The system should also allow the physicist to spend only a minimal time for a particular PSQA process, data analysis and generation of the report. Despite the significance of PSQA for CK

patients, little to no research has been conducted and very few researchers addressed this matter up to this date. Hence, there is a lack of a proper 3D PSQA system that can adequately meet the above-mentioned requirements. Polymer gel is one of the most promising high resolution 3D dosimetry systems for PSQA in SRS/SRT/SBRT that can offer those capabilities. The assessment can be performed experimentally and can be used for the comparison and verification of dose calculations for 3D volume irradiation that is prepared for the treatment of cancer patients using standard treatment planning systems (TPS). The reusability of the polymer gel dosimeters could be another important feature to improve the efficiency.

1.3 Research Objectives

This study aims to evaluate the FOFs and the performance of a 3D PSQA system as applied to the CK radiotherapy/radiosurgery system. The specific objectives of the study are as follows:

1. To calculate the FOF for the CK system by using several commercially available detectors, radiochromic films and high resolution 3D polymer gel dosimeters.
2. To compare the corrected FOF data from all the studied detectors with the MC simulation data.
3. To evaluate the performance of a new 3D gel based PSQA system using 3D gamma evaluation method for various CK treatment plans by comparing with 2D gamma evaluation of EBT3 films as reference.

1.4 Scope of Research

This research would study a series of commercially available detectors to measure FOFs for the CK system. The measured raw output factors were corrected by

applying the field output correction factors that were recommended and tabulated by IAEA TRS 483 so that data can be gathered to establish standard FOF database for CK system. In addition, MC simulation and 3D gel dosimeters using spectrophotometry were studied to measure FOFs for new detectors or procedures for CK.

For CK PSQA, the required features such as high resolution and 3D capability were introduced and studied in the prototype CrystalBall gel system (Maryanski 2018). Its first commercial model and VOLQA analysis software were used for PSQA for CK patients in this study. The validation of the CrystalBall-VOLQA system was accomplished by comparing gamma evaluation results of the PSQA with that from EBT3 film irradiations in 2D planes for the same patient plans.

1.5 Thesis Outline

The thesis consists of five chapters. Chapter 1 discusses briefly external beam radiation therapy, the CK robotic radiotherapy/radiosurgery system output factor and PSQA. The problem statements, research objectives and scope of the research are also discussed in this chapter. Chapter 2 contains the theoretical background for the absolute, reference and relative dosimetry along with FOFs and PSQA for the CK system. A literature review of the relevant studies is also described in this chapter. Chapter 3 discusses the materials and methods that are employed in this research. This involved the experimental setup, measurements and simulation of FOFs for the CK system. A new 3D gel PSQA phantom setup and procedures for CK patients are also discussed in this chapter. Chapter 4 discusses the results of all measurements and experiments that are performed in this study. Uncertainty for the measurements are also discussed at the beginning of this chapter. Finally, the conclusion of this study is presented in Chapter 5. The recommendations for the related future works are also stated in this chapter.

CHAPTER 2

LITERATURE REVIEW

In this chapter, the aim is to discuss the LINAC, CK radiotherapy/radiosurgery system and its use in the treatment of cancer patients, small field detectors, and some other key dosimetric parameters. The focuses are on the measurements and verification of FOFs and PSQA for the CK system.

2.1 Radiation Therapy

A LINAC is commonly used to deliver the high energy beam of radiation to the tumor for treatment in radiation therapy. Radiation therapy techniques have improved significantly over time and the advancement of technology has greatly impacted the treatment of cancer.

2.1.1 Linear Accelerator for Radiation Therapy

A LINAC is a device that is used to produce high-energy x-rays or electrons. It accelerates subatomic particles such as electrons to high energies through an accelerator tube using high frequency electromagnetic waves (Khan, 2010). One of the applications of LINACs is to produce high energy x-rays for cancer treatments. The high energy electrons from the accelerator tube are directed to hit a high atomic number metal target. The collision produces x-rays that can be filtered and collimated to obtain desired beam characteristics. The medical LINAC is commonly used to administer external beam radiation treatments to cancer patients during radiation therapy, also known as external beam radiation therapy. The high-energy x-ray or electron beams can be customized by the LINAC to precisely and accurately fit the shape and size of the tumor. This way, the cancer cells are destroyed while the adjacent healthy tissues are spared (Chang et al., 2004). A medical LINAC that is used in

radiation therapy usually consists of several components such as a wave-guide, a target, a gantry, a collimator and a treatment couch (Mallick et al., 2020). Figure 2.1 shows the schematic diagram of the components of a typical medical LINAC used for radiation therapy.

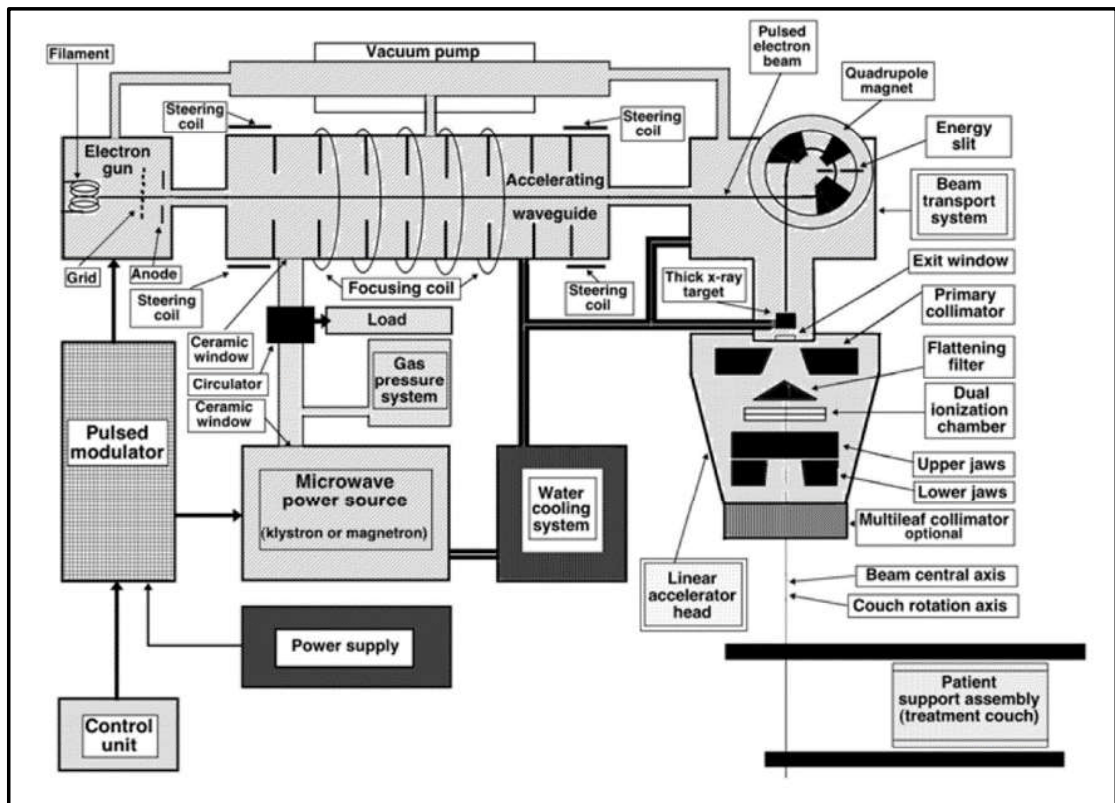


Figure 2.1: Schematic diagram of the main components of a typical medical LINAC (adapted from Podgoršak, EB. Radiation Physics for Medical Physicists. Springer-Verlag Berlin Heidelberg, 2006).

In order to target the tumor, the gantry rotates around the patient directs the x-rays from various angles. The collimator is used to shapes the radiation beam to conform to the tumor's outline. The treatment couch moves the patient into correct position and adjusts the height and angle as desired (RadiologyInfo.org for patients, 2023). A radiation therapist operates the LINAC and follows a treatment plan which is generated by a radiation oncology physicist or a radiation dosimetrist by following the prescription from a radiation oncologist (American Cancer Society, 2023). The radiation dosage, frequency and duration of the radiation therapy are all specified in

the treatment plan. Throughout the session, the radiation therapist also monitors safety and comfort of the patient.

2.1.2 CyberKnife System for Radiation Therapy

Radiation therapy technology has evolved significantly since its first use in more than a hundred years. One of the latest advancements in this field is the robotic CK system (Figure 2.2), which came into treatment in the 1990s (Adler, 1993; 1996) in Stanford, USA. The main components of the system are shown in Figure 2.3. The system was developed to facilitate the treatment of image-guided SRS/SRT/SBRT. It uses a compact LINAC with an X-band (~ 9 GHz) cavity magnetron and a side-coupled standing wave waveguide that accelerates electron to deliver a flattening-filter (FFF) 6 MV photon beam (Kilby et al., 2010; Moignier et al., 2014; Aslian et al., 2020). The LINAC is mounted on a robotic manipulator (Kuka Roboter GmbH, Ausberg, Germany) which possess a position repeatability of around 0.10 mm. The robotic manipulator possesses six degrees of freedom that allows it to position within a large three-dimensional (3D) workspace around the patient in a highly precise manner. It can direct each treatment beam usually in a non-coplanar point in space (Kilby et al., 2010). Unlike the fixed gantry LINACs, the ambulatory capability of the robotic manipulator enables it to deliver radiation beams from more than 1200 accessible field directions (Hara et al., 2007). The delivery of nonisocentric beam offers the best possible dose conformity while maintaining dose uniformity. During treatment, the patient is positioned on a robotic couch that may move on three translational and three rotational axes (if required) for patient setup. The system offers 12 circular fixed cones with discrete diameter ranging from 0.50 cm to 6.00 cm (0.5, 0.75, 1.0, 1.25, 1.5, 2.0, 2.5, 3.0, 3.5, 4.0, 5.0, and 6.0 cm) or alternatively a dodecagonal-shaped variable aperture collimator field named IrisTM with the same set of twelve field sizes (Echner

et al., 2009; Fasola et al., 2015). The treatment is delivered by using a single or some combinations of the fixed cones or IrisTM aperture sizes at a nominal 80 cm source-to-axis distance (SAD). In 2013, Accuray incorporated multileaf collimator (MLC) technology, named InCiseTM, into the CK system which consists of 41 leaf pairs with a width of 2.5 mm each (Fürwegera et al., 2016; Jang et al., 2016; Ding et al., 2018). With a maximum field size of 12 cm × 10.25 cm, the device allows adjustable field shaping to conform to the shape of the tumor (Fürwegera et al., 2016). A new MLC system (InCiseTM 2) was introduced in 2015 with 52 leaf pairs (Asmerom et al., 2016).



Figure 2.2: A typical CK modality (Accuray VSI system used for this study).

The CK system uses image guided radiotherapy (IGRT) technique to track the tumor accurately and precisely. Depending on the treatment site and functional need, the system uses one of the several tracking methods available, such as 6D skull, Spine tracking, fiducial tracking, or synchrony for image guidance (Kilby et al., 2010; Ding et al., 2018). An orthogonal pair of kilovoltage x-ray imaging sources (fixed on the

ceiling) and flat panel detectors make up the image guided system. The amorphous silicon flat panel detector pairs are installed in the floor and positioned on either side of the patient to capture a pair of orthogonal real-time, high resolution, digital x-ray images from the source with a field size of 20 cm × 20 cm (Fasola et al., 2015). The registration is performed by superimposing the orthogonal x-ray images with the digitally reconstructed radiographs (DRR) of implanted fiducials or bony anatomical structure of the patient that are obtained from CT image sets of the patient. Each of the two image sets are precisely aligned by assessing and minimizing the differences in three translational and three rotational axes. When the alignment of the two sets is within the acceptable limit, the plan is allowed to be ready for treatment delivery. Accurate targeting of the LINAC is achieved through precise adjustments of treatment couch and the robotic manipulator. Stereotactic precision is preserved by repeating this procedure at user selected time intervals during the entire course of treatment.

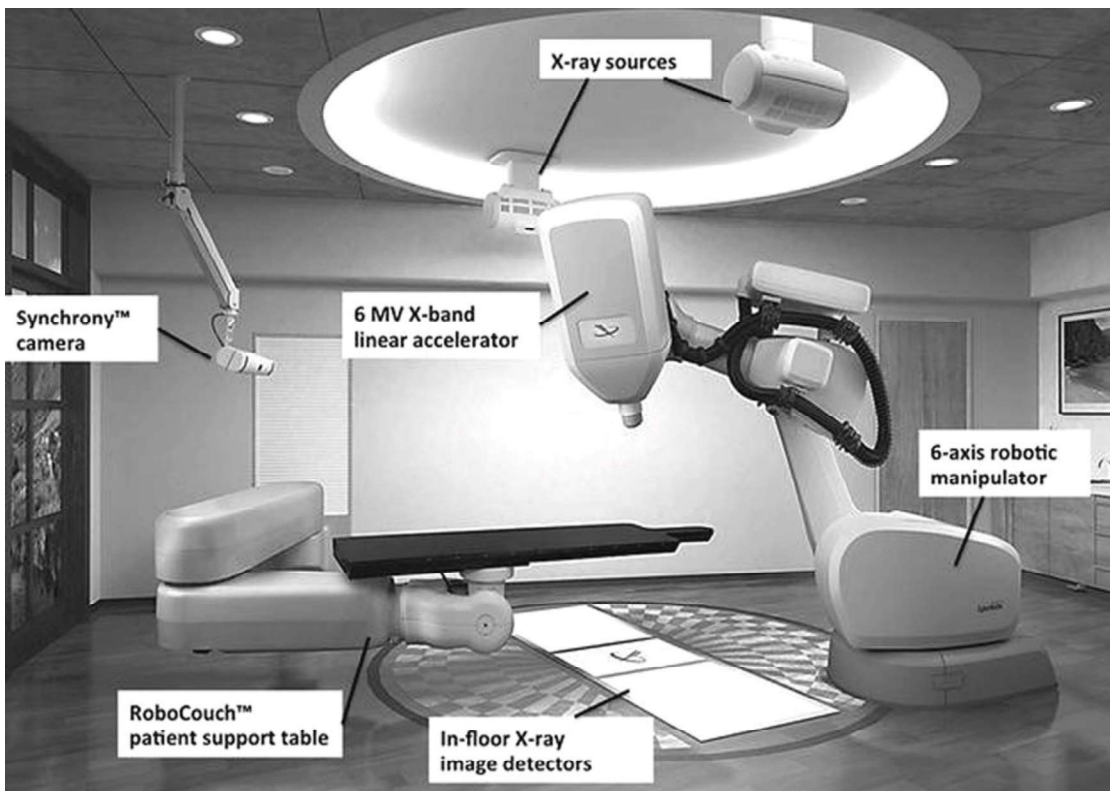


Figure 2.3: Main components of CK system (adapted from Fasola et al., 2015).

2.1.3 Absorbed Dose

When an ionizing radiation passes through a medium, it interacts with the medium and a part or entire energy of the radiation is transferred to the medium. Absorbed dose is the measure of the amount of energy deposited in a medium by ionizing radiation. The absorbed dose is expressed in terms of the energy imparted, ϵ (ICRU Report-33, 1980). Hence, the absorbed dose (D) is defined as the energy imparted per unit mass (m) of the medium by the ionizing radiation as follows:

$$D = \frac{d\epsilon}{dm} \quad (2.1)$$

The energy imparted is measured in the unit Joule (J) while the mass of the medium is measured in the unit kilogram (Kg). Usually, the absorbed dose is measured using SI unit of Gray (Gy), where:

$$1 \text{ Gy} = 1 \text{ Joule/Kg}$$

The absorbed dose was originally calculated using another unit as radiation absorbed dose (rad). The relationship between Gy and rad is:

$$1 \text{ Gy} = 100 \text{ rad}$$

The biological effects of radiation on body are not directly correlated with the absorbed dose. Different types or quality of radiation may induce varying levels of damage for the same absorbed dose. Therefore, often a radiation weighting factor is introduced to obtain an equivalent dose, which reflects the relative biological effectiveness of the radiation quality (Hall et al., 2006).

2.1.4 Absolute, Reference and Relative Dosimetry

The concepts of absolute, reference and relative dosimetry are very common terms that are routinely and frequently used in radiotherapy physics. They are discussed briefly in the following paragraphs.

2.1.4 (a) Absolute dosimetry

Absolute dosimetry refers to the measurement of a dosimetric quantity with an instrument of the highest metrological quality. It is a method of measuring the amount of radiation delivered to a specific point in a material or tissue under standard conditions without the need for calibration of dosimeter response. It is an essential tool for ensuring the quality and safety of radiation therapy, diagnostic imaging, and industrial applications. Absolute dosimetry requires accurate calibration of the instruments and methods used to measure the dose, as well as careful consideration of the environmental and physical factors that may affect the results (Andreo et al. (2017)). It can be performed using various techniques using various detectors such as ionization chambers, thermoluminescent dosimeters, radiochromic films, calorimeters, and chemical dosimeters. Each technique has its own advantages and limitations, depending on the type and energy of the radiation, the dose range, and the desired accuracy and precision. For radiotherapy, exposure or dose measurements with an instrument is considered to be absolute dosimetry (de Almeida et al., 2022). The reference influence quantities (temperature, pressure, applied voltage etc.) are recorded and reported.

In general, absolute dosimetry is carried out in Primary Standard Dosimetry Laboratories (PSDL). PSDLs are standardizing laboratories designated by a national or international authority for the purpose of developing, maintaining and improving

primary standards in radiation dosimetry (IAEA, 1998-2023). Those laboratories use instruments with the highest metrological quality (De Almeida et al., 2022). Those laboratories are capable of measuring the quantities according to their definition. They use highly sophisticated equipments and procedures to reach the level of standards. The National Institute of Standards and Technology (NIST) in the United States, the National Physical Laboratory (NPL) in the United Kingdom, and the Physikalisch-Technische Bundesanstalt (PTB) in Germany are few examples of PSDLs.

2.1.4 (b) Reference dosimetry

Reference dosimetry refers to the measurement of the dosimetric quantity in the user's Institution. Reference dosimetry is essential for ensuring the quality and safety of radiotherapy treatments. It is usually the process of measuring absorbed dose in water with an ionization chamber for a radiation beam. It is used to calibrate and verify the dose that will be delivered to a radiotherapy patient. Reference dosimetry requires accurate and precise measurements that are traceable to the standards established by the international metrological network (De Almeida et al., 2022). The reference conditions used in the calibration laboratory during calibration of the ionization chamber must be reproduced in the user's institution. Hence, it is essential for the user to measure the influence quantities (temperature, pressure, applied voltage etc.) at the time of acquisition and correct the acquired data accordingly using the correction factors obtained (from the influence parameters). Reference dosimetry also involves the implementation of correction factors to account for the differences between the calibration and measurement conditions, such as beam quality, polarity, recombination and chamber orientation (De Almeida et al. 2022).

2.1.4 (c) Relative dosimetry

Relative dosimetry is a method of measuring the dose of radiation relative to a reference dose. Relative dosimetry is used to verify the accuracy and consistency of radiation therapy treatments, as well as to calibrate radiation detectors and dosimeters. In a clinical setting, a variety of measurements are performed under non-reference conditions where the calibration conditions do not need to be reproduced or introduced because are relative to some specific values of the same measurement. Those measurements are referred to as relative measurements or dosimetry that include depth dose, tissue phantom ratio, profiles, output factors, etc. It is possible to conduct those measurements using a variety of detectors and still ensure that their values are consistent with the actual value of the quantity. Relative dosimetry can be performed using ionization chambers, thermoluminescent dosimeters, film dosimetry, or gel dosimetry. The characteristics of those detectors such as sensitivity, short-term repeatability, long-term stability, angular, dose rate and energy dependence, detector size, leakage, signal fading, etc. must be considered during the measurements (de Almeida et al., 2022).

Table 2.1: The summary on the concepts of absolute, reference and relative dosimetry in different aspects.

Aspects	Absolute Dosimetry	Reference Dosimetry	Relative Dosimetry
Definition	Measurement of a quantity in accordance with its definition	Reference dosimetry compares a quantity to an absolute reference	Measure of a quantity relative to a reference point or standards
Place	PSDL or SSDL	User Institution under user beam quality	User Institution under user beam quality
Calibration	Done under control of standard conditions	Calibration coefficient need to be used	Calibration coefficient need not to be used
Accuracy level	Higher accuracy	Higher accuracy	May have lower accuracy

Table 2.1. Continued.

Aspects	Absolute Dosimetry	Reference Dosimetry	Relative Dosimetry
Complexity	Complex and time consuming	Complex	Generally simple
Reference conditions	Done with controlled reference conditions	Reference conditions used in calibration laboratory must be reproduced	Reference conditions Need not to be applied
Correction of influence quantities	Done under controlled influence quantities	Need to correct for influence quantities	No Need to correct for influence quantities
Instruments	Ionization chamber	Dosimeters that have been calibrated against a primary standard	TLDS, diodes, film, MOSFET, detector arrays, etc.
Application	Commonly used in high-precision radiotherapy applications	Used in calibration of treatment machines	Widely used in routine quality assurance, dose verification, assessment of dose distribution, etc.
Example	Measurement of Exposure or absolute dose to a medium	Measurement of Exposure or dose to a medium under user beam quality	OF, PDD, TPR, OCR, TMR, etc.

2.1.5 Small Field Detectors

The physical and dosimetric characteristics of some of the detectors used in this study are discussed briefly in the following paragraphs.

2.1.5 (a) Ionization Chamber

An ionization chamber is a gas-filled radiation detector. An external electric field in the active volume of the chamber causes direct ionization of the air or gas upon exposure to radiation. The created charges are by two electrodes inside the volume. Ionization chambers possess very good stability and linear dose-response. They are also free of directional dependency due to the spherical shape of the sensitive volume

(Low et al., 2011). Although they are used in radiation dosimetry, due to their relatively large size or volume, most of the ion chambers introduce volume averaging effects that limits their use in dosimetry of small fields (Das et al., 2000; Low et al., 2003). Nonetheless, PinPoint ionization chambers (Figure 2.4) that have sensitive volume $<0.1 \text{ cm}^3$ are used to measure different parameters of small fields (Low et al., 2011; Pantelis et al., 2012; Manavalan et al., 2021).



Figure 2.4: A PinPoint ionization chamber (PTW-Freiburg, Germany).

2.1.5 (b) Diode Detectors

The silicon diode detector is a type of p-n junction, which is a region on a boundary between n-type and p-type silicon. Upon irradiation, it creates extra minority charge carriers in the n- and p- sides of the silicon. These charge carriers move toward the p-n junction by diffusion. The induced radiation current can be measured by collecting the charge carriers within diffusion length distance from the junction. The silicon diodes require an energy of 3.6 eV to create an electron-hole pair (Parwaie et al, 2018). This energy to generate an ion pair is much smaller than that required by an ionization chamber. Therefore, the sensitivity of diodes is higher than that of ionization chambers (Silva, 2015). Due to their relatively small size, high spatial resolution and

superior dose response, diode detectors are suitable for small field dosimetry (Eklud and Ahnesjö, 2010). Nonetheless, these detectors (Figure 2.5) have disadvantages of dependence on temperature, energy and dose-rate (Low et al., 2003; Pappas et al., 2008; Jursinic, 2009; Eklud and Ahnesjö, 2010; Pantelis et al., 2012; Reggiori et al., 2016; Biasi et al., 2018; Manavalan et al., 2021). Edge detector is a diode detector constructed by Sun Nuclear Corporation, USA.



Figure 2.5: A PTW diode (PTW- Freiburg, Germany).

2.1.5 (c) Diamond Detectors

Diamond detectors (Figure 2.6) exhibit tissue equivalent properties. Because of their small volume, high dose-response, energy independence and directional independence, they become suitable for small field measurements (Heydarian et al., 1996; Das et al., 2000; Pappas et al., 2008; Larraga-Gutierrez et al., 2015). The sensitive volume of the natural diamond detectors is natural diamond. When a particle passes through the detector, a linear charge density is ionized to produce electron-hole pairs; as a result, a current will be induced. The induced current signal is amplified and collected through electrodes where an external electric field is applied. The ionization energy for diamond is 13 eV/ion-pair (Ravichandran et al., 2016) that is also much

lower than the energy required to generate an ion pair in ionization chambers. Some of the drawbacks of natural diamond detectors include their high cost, non-reproducibility and relatively large volume for small field measurements (Marsolat et al., 2013).



Figure 2.6: A PTW natural diamond detector (PTW- Freiburg, Germany).

Synthetic chemical vapour deposition (CVD) based single crystal diamond dosimeter (SCDDo) or polycrystalline diamond detectors have a sub-micron thick diamond layer(s) that can tolerate high electric field gradient (Fidanzio et al., 2005; Manavalan et al., 2021). Both types of diamond detectors have applications in various measurements in radiotherapy including small fields for CK (Fidanzio et al., 2000; 2005; Tranchant et al., 2008; Tromson et al., 2008; Almaviva et al., 2009; Rebisz-Pomorska et al., 2009; Schirru et al., 2010; Betzel et al. 2012; Ciancaglioni et al., 2012; Marsolat et al., 2013; Chalkley and Heyes, 2014; Ravichandran et al., 2016; Manavalan et al., 2021; Talamonti et al., 2021). However, natural diamond detectors have significant dose rate dependency (Hoban et al., 1994; De Angelis et al., 2002). In order to compensate for this drawback, their readings need to be corrected with appropriate correction factors (Laub et al., 1999; Sauer and Wilbert, 2007). Synthetic diamond detectors do not show significant dose rate dependency, however, for small

field, they show over-response for relative field factors measurements (Marsolat et al., 2013; O'Brien et al., 2016). Consequently, the readings obtained with these detectors should also be corrected by using an appropriate correction factor.

2.1.5 (d) Scintillation Detectors

Scintillation detector works by using special crystals that emit light upon irradiation. The sensitive volume of a plastic scintillation detector (PSD) is a scintillating fibre. This fibre emits scintillation photons (light) when irradiated. A light pipe (optical fibre) is used to transmit the scintillation photons to a photodetector that converts lights to electric signals to be read out by an electrometer. The amount of light photons is proportionally correlated with the irradiation dose. PSDs (Figure 2.7) are nearly tissue equivalent (Beddar et al., 1992; Dimitriadis et al., 2017). They possess enhanced spatial resolution and are unaffected by dose rate, energy, and temperature (Beddar et al., 1992; Archambault et al., 2005; Beddar 2006; Dimitriadis et al., 2017 Galvasis et al., 2019;). One of the disadvantages in using PSDs for radiation measurements is the production of Cherenkov light radiation when the optical fibre is exposed to radiation. In order to obtain the correct reading, the Cherenkov radiation should be subtracted from the raw PSD signal (Archambault et al., 2006). Different methods are employed to filter out the Cherenkov signal from the readout. PSDs are used for various dosimetric measurements (Beddar et al., 1992; Archambault et al., 2005; 2006; Gagnon et al., 2012; Morin et al., 2013; Carrasco et al., 2015; Underwood et al., 2015; Burke 2017; Pasquino et al., 2017), but they are still not widely adopted in a routinely practice. However, W1 type of PSDs from Standard Imaging Inc. (Madison, WI, USA) have been employed for measuring point doses (Pasquino et al., 2017). W2 type PSDs are used to measure point doses as well as relative scanning (Galvasis et al., 2019). Several authors have also investigated PSDs for dosimetry of

small fields (Qin et al., 2016; Mancosu et al., 2017; Xue et al., 2017; Debnath et al., 2020).

Three PSDs (Standard Imaging Inc., Madison, WI, USA); one Extradin W1 type and two W2 type (with dimensions: 1 mm diameter \times 1 mm long and 1 mm diameter \times 3 mm long, respectively), were used to measure and calculate the FOF for CK. The measurements from the PSDs were corrected accordingly from the Cherenkov radiation by following the guidelines provided by the vendor. The field output correction factors for small field dosimetric measurements with Extradin W1 and W2 type PSDs were found to be nearly equal to unity (Beddar 2006; Alfonso et al., 2017; Galvasis et al., 2019; Carrasco et al., 2015; Pasquino et al., 2017). Therefore, no field output correction factors were applied to the measurement ratio to obtain the FOFs for those PSDs used.

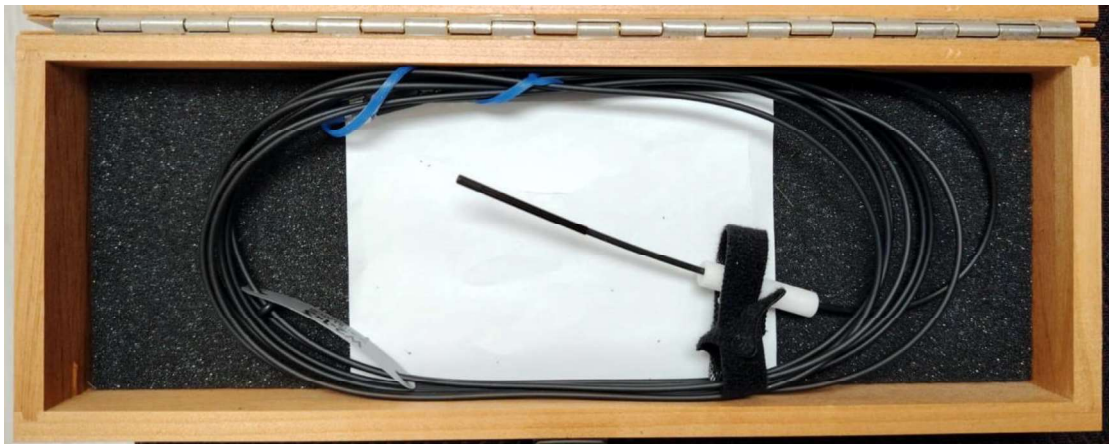


Figure 2.7: An Extradin W2 Scintillation detector (Standard Imaging, Inc., Madison, WI, USA).

Table 2.1 below shows the summary of different physical characteristics for the discussed small field detectors used for this study.